

Asymmetric impacts of dryness and wetness on tree growth and forest coverage

Shan Gao^{a,b,c,*}, Tao Zhou^{b,c,*}, Chuixiang Yi^{d,e}, Peijun Shi^{b,c}, Wei Fang^d, Ruishun Liu^f, Eryuan Liang^{a,g}, J. Julio Camarero^h

^a Key Laboratory of Alpine Ecology, Institute of Tibetan Plateau Research, Chinese Academy of Sciences, Beijing 100101, China

^b State Key Laboratory of Earth Surface Processes and Resource Ecology, Faculty of Geographical Science, Beijing Normal University, Beijing 100875, China

^c Key Laboratory of Environmental Change and Natural Disaster of Ministry of Education, Academy of Disaster Reduction and Emergency Management, Beijing Normal University, Beijing 100875, China

^d School of Earth and Environmental Sciences, Queens College, City University of New York, Queens, NY 11367, USA

^e Earth and Environmental Sciences Department, the Graduate Center of the City University of New York, New York, NY 10016, USA

^f Key Laboratory of Tibetan Environmental Changes and Land Surface Processes, Institute of Tibetan Plateau Research, Chinese Academy of Sciences, Beijing 100101, China

^g Center for Excellence in Tibetan Plateau Earth Sciences, Chinese Academy of Sciences, Beijing 100101, China

^h Instituto Pirenaico de Ecología (IPE-CSIC), 50059 Zaragoza, Spain

ARTICLE INFO

Keywords:

Forest coverage
Legacy effects
Natural experiment
Temporal dynamics
Tree-ring
The southwest USA

ABSTRACT

The prevalence of legacy effects, especially in drought-prone forests, makes the accurate assessment of forest dynamics under frequent climate fluctuations challenging. Here, we investigated the dynamic impacts of inter-annual water deficit on both tree radial growth and forest coverage in the southwest USA. We designed a series of regional-scaled “natural experiments”, specifically, we preset hypothetical water conditions of current- and antecedent-hydrological years and conducted quantitative analysis on grouped tree-ring records and sub-pixel changes of forest coverage under these conditions. Results showed that the temporal patterns of growth legacy changed dynamically when studying it on multiple events level (i.e., both past and current climate condition are taken into consideration): under current-hydrological year dry conditions, legacy effects over 3 years could be detected; while under current-hydrological year wet conditions, only previous 1 year's legacy could be detected, and its intensity was only 57% of that under current-hydrological year dry conditions. Furthermore, our results revealed that growth dynamics observed in tree rings were not fully consistent with the dynamic of forest coverage. Wetness enhanced growth pronouncedly, whereas normal to wet conditions only barely maintained the stability of forest coverage, suggesting that tree growth is more sensitive to wetness than forest coverage. In addition, the impact of consecutive dry years on tree radial growth showed no significant difference from that of a single dry year, but the decline of forest coverage accelerated after consecutive droughts. A possible explanation is that trees sampled from environmentally harsh locations though climate sensitive are not subjected to strong competitive constraints. These findings suggest that examining the responses at multiple scales in forests can help us gain more comprehensive understanding of processes involved in forest dynamics.

1. Introduction

Forest ecosystems are becoming increasingly vulnerable in the face of climate change, especially in semiarid regions (Allen et al., 2010, 2015; Anderegg et al., 2012; D'Orangeville et al., 2018; Liang et al., 2016; Williams et al., 2010a). Intensified drought stress, now generally agreed upon as the most widespread and frequent threat to many forests, has led to recent higher tree mortality rate and forest die-off

episodes (Allen et al., 2010; 2015; Anderegg et al., 2012; Camarero et al., 2015; Cook et al., 2015; Reichstein et al., 2013). Although a meteorological water budget can be constantly monitored, its impacts on tree growth and forest dynamics are quite uncertain. One important reason is the pervasive existence of legacies (i.e. the lagged responses to extreme events) in forest ecosystems (Anderegg et al., 2015; Huang et al., 2018; Jiang et al., 2019; Peltier et al., 2016; Reichstein et al., 2013; Wu et al., 2017).

* Corresponding authors.

E-mail addresses: gaoshan@itpcas.ac.cn (S. Gao), tzhou@bnu.edu.cn (T. Zhou).

<https://doi.org/10.1016/j.agrformet.2020.107980>

Received 23 September 2019; Received in revised form 12 March 2020; Accepted 13 March 2020

0168-1923/ © 2020 Elsevier B.V. All rights reserved.

Observational research generally revealed 1- to 4-year long legacies recorded in tree-rings at regional to global scales and presented the recovery process of tree growth after droughts (Anderegg et al., 2015; Gazol et al., 2017; Huang et al., 2018; Peltier et al., 2016; Wu et al., 2017). Similarly, the enhancement of radial growth after extreme wetness could also be observed for 1 to 5 years (Jiang et al., 2019). So far, most related studies focused on lagged impacts of past extreme years or events on current growth; however, current water condition immediately influence current growth, which may alter or offset the ecological impacts of past extremes (Ryo et al., 2019). For instance, the North American monsoon can reduce the negative impacts on tree growth caused by dry La Niña winters (Peltier and Ogle, 2019). However, we still lack a comprehensive understanding of the temporal dynamics of legacy effects when both past and current climate condition are taken into consideration.

In addition, despite the abundance of evidence on the significant legacy effects recorded in tree-rings, whether these growth legacies could be upscaled to the level of a whole forest have not been fully discussed. Tree-ring width is a direct measurement of a tree's radial growth, and ring width indices (RWI), which are the standardization of tree-ring width chronology after removing age-related growth trend, have been considered as a reliable indicator of the variability of forest growth as well as aboveground woody biomass (e.g., Zweifel et al., 2010). Many tree-ring chronologies contributed to the International Tree-Ring Data Bank (ITRDB) were developed from tree cores of old and dominant individuals for extracting long-term climate signals (Cook et al., 1995), yet their representativeness was less considered (Babst et al., 2018; Klesse et al., 2018; Zhao et al., 2018). In a forest, trees' size, age, competition intensity, microenvironment and other factors may all affect their sensitivity to climate and susceptibility to drought-triggered mortality (Camarero et al., 2018; Larson et al., 2015; Liu et al., 2018; McDowell and Allen, 2015; Preisler et al., 2019; Xu et al., 2018). Comparing the legacy effects over multiple years at both individual tree/plot scale and entire forest/landscape level would provide comprehensive information of forest ecosystems undergoing climate change and help to address uncertainties at both scales (Hartmann et al., 2018).

In this study, we (1) examined the temporal dynamics of legacy effects recorded in tree-rings with the consideration of both past and current water deficit conditions, and (2) compared legacy effects on both tree-ring widths and forest coverage change to expand our understanding of forest dynamics in response to climate from both spatial scales. We hypothesized that the temporal pattern of legacy effect changes when effects from multiple years are superimposed on top of one another. We also hypothesized that the response of tree growth to the shift of interannual water deficit condition is rapid and intense, but forest coverage does not have obvious changes in a short period. To test our hypotheses, we designed a series of regional-scaled “natural experiments” using tree-ring width data and forest coverage data. We analyzed the water deficit legacies of three antecedent hydrological years before current-hydrological years (ybc) on tree-ring widths under different water deficit conditions during the current-hydrological years. The term “current-hydrological years” refers to the hydrological years (i.e., beginning in October of the previous year and ending in September of the current year in the case of the northern Hemisphere) when corresponding tree-rings were formed. A similar method was also used to explore dynamic changes of forest coverage, so that response differences between tree growth and forest coverage to different interannual water deficit conditions could be revealed.

2. Materials and methods

2.1. Study region

The study region is in the southwestern United States that includes the states of Utah, Colorado, Arizona, and New Mexico (Fig. 1). The

regional climate of the Colorado Plateau is dependent on large-scale effects such as wind direction and rain-shadow from the Sierra Nevada, and largely influenced by elevation and topography (Allen et al., 1998). It has large spatial gradients in both temperature and precipitation (Biederman et al., 2017): low elevation is an arid desert climate, while higher elevations feature alpine climates with large tracts of high-elevation forests. Large interannual variability in precipitation characterizes this region, as it is influenced by the El Niño Southern Oscillation and the Pacific Decadal Oscillation. Recurring droughts are the primary limiting factor to tree growth in most of this region's forests (Leavitt et al., 2011; Williams et al., 2010a).

We chose the southwest USA as our study region for several reasons. First of all, delayed impacts of water deficit are prevalent, and forests are vulnerable to further droughts in dry ecosystems (Anderegg et al., 2015). Secondly, tree-ring sampled sites are distributed densely in the region. Besides, the scarce soil water and meager organic matter here cannot buffer the impacts on tree growth from water stress (Swetnam and Betancourt, 1998), which reduces a possible source of bias in our study.

2.2. Tree-ring data

A total of 357 tree-ring width chronologies of three major tree species (*Pinus edulis* Engelm., *Pinus ponderosa* Douglas ex C. Lawson and *Pseudotsuga menziesii* (Mirb.) Franco) were obtained from the International Tree-Ring Data Bank (<https://www.ncdc.noaa.gov/data-access/paleoclimatology-data/datasets/tree-ring>; Fig. 1, Table S1). To transform tree-ring width data into ring-width indices (RWI), long-term trends caused by aging and increasing trunk diameter were mostly removed by negative exponential curves using the ARSTAN program (Cook, 1985). We chose to use standard chronologies since they do not contain the age-related trend yet still have autocorrelation (the effect of previous climate or growth on the current year's growth) included. After performing this standardization, all chronologies were scaled to a standard mean (RWI = 1000) with a comparable variance; in this way, spatial heterogeneity among these tree-ring sites could be largely reduced. Processed chronologies after the year 1902 were selected for further analyses.

The tree-ring database we used was composed of 357 standard chronologies of three major species in the study region, spanning from 1902 to 2012, resulting in a total of 29,969 site-years. Each site-year was considered as an individual specimen potentially impacted by local climate variations. Tree growth increment patterns across species and space were generally coherent (Williams et al., 2012). The three species have similar responses to water deficit, so we pulled them together to perform analyses (Figure S1).

2.3. Forest coverage change data

Forest cover data of the study region were extracted from MODIS Land Cover Climate Modeling Grid (MCD12C1) version 6 data product (yearly gridded data with a spatial resolution of 0.05°), International Geosphere-Biosphere Program (IGBP) classification scheme. In the classification scheme, 17 land cover classes were identified along with their sub-pixel proportions. Sub-pixel proportions of each land cover class in each 0.05° pixel ranges from 0 to 100%, thus the sub-pixel resolution could be considered as 0.005° (approximate 560 m). Forest categories are determined where lands dominated by woody vegetation with a percent cover over 60% and height exceeding 2 m (Friedl and Sulla-Menashe, 2015). We summed the sub-pixel proportions of forest categories (i.e. evergreen needleleaf forests, evergreen broadleaf forests, deciduous needleleaf forests, deciduous broadleaf forests and mixed forests) for each pixel in each year from 2001 to 2017 as forest coverage (FC) data. During the period, if forest ever appeared in a pixel (i.e. the number of years which identified forest coverage larger than 0, equal to or greater than one), then we considered the pixel as a

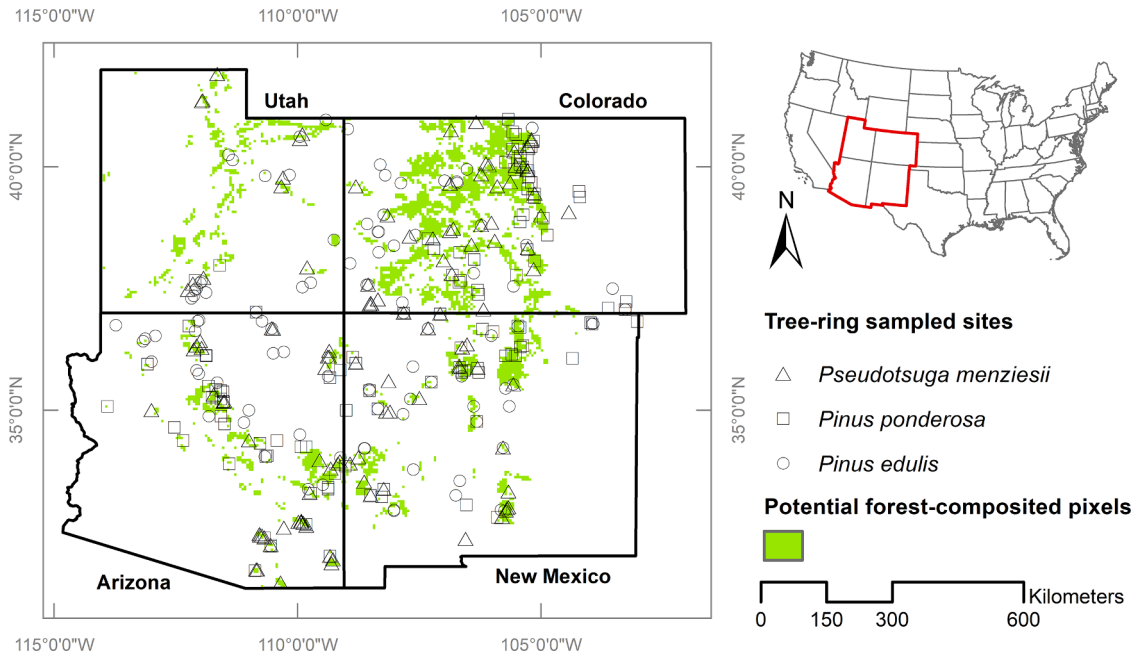


Fig. 1. Distribution of tree-ring chronologies used in southwest USA. A total of 357 tree-ring chronologies of three major tree species (*Pseudotsuga menziesii*, *Pinus ponderosa*, *Pinus edulis*) were included. Green pixels indicate “potential forest composited pixels (PFPs)”.

“potential forest composited pixel (PFP)”. The map of PFPs within the study region is presented in Fig. 1. The distribution of FC data within PFPs is displayed in Figure S2. Most of FC data were less than 10%.

Forest coverage change (FCC) was calculated as the departure of sub-pixel forest coverage (FC) of the current year from its previous year (Eq. (1)):

$$FCC_j^n = FC_j^n - FC_j^{n-1}, \quad (1)$$

where j represents the j th PFP, and n represents the n th year.

The study region contained 3388 PFPs, spanning from 2002 to 2017, resulting in a total of 54,208 FCC data.

2.4. Climate data

Monthly gridded (0.5° resolution) climate data—precipitation (P_m) and potential evapotranspiration (PET_m)—from 1901 to 2017 for each pixel with tree-ring chronologies as well as PFPs were obtained from the Climate Research Unit, TS v.4.01 (<https://crudata.uea.ac.uk/cru/data/hrg/>). We first calculated monthly water deficit (D_m) of each site (Eq. (2)) and aggregated into their annual scale (D_y). “Annual” in this study refers to the hydrological year (Fang et al., 2015; Salzer and Kipfmüller, 2005; Williams et al., 2010b), which presents a more reasonable correspondence between hydrological processes and tree phenology.

We used annual water deficit anomaly (D_{ya}) to explore the impact of water deficit variability on tree radial growth and growth legacies. It was these differences that likely influence subsequent growth, thus using water deficit anomalies provides a standardization across sites and years and allows meaningful comparisons.

$$D_{mj}^i = P_{mj}^i - PET_{mj}^i, \quad (2)$$

$$D_{yj} = \sum_{i=1}^{12} D_{mj}^i, \quad (3)$$

$$D_{ya_j}^n = D_{yj}^n - \overline{D_{yj}}, \quad (4)$$

where i represents the i th month of a hydrological year, j represents the j th tree-ring sampled site, n represents the n th hydrological year, and

$\overline{D_y}$ represents the mean water deficit averaged over 111-hydrological years (i.e., for 1902–2012).

We matched gridded D_{ya} to RWIs. For tree-ring chronologies within the same grid, we averaged them for each year to reduce bias caused by the rough resolution of climate data.

2.5. Natural experiments design

2.5.1. To investigate water deficit legacies in tree-ring widths

Natural experiments are observational studies, yet they share a major attribute of controlled experiments—that is, comparisons of outcomes across treatment and control conditions, which pave the way for causal inference (Dunning, 2008, 2012; Gao et al., 2018). In a natural experiment, individuals (or clusters of individuals) are exposed to the treatment and control conditions that are determined by nature, but the process governing the exposures should arguably resemble random assignment (Dunning, 2012). We considered tree-ring formation in natural conditions resembles a randomized exposure. With abundant RWI data, we designed “natural experiments” to study the legacy effects of various water deficit conditions in previous hydrological years on tree radial growth of the current years. The two key steps for revealing the legacy effects of target years (the n^{th} ybc (with $n = 3, 2, 1$)) on current tree radial growth were (1) differentiating the three water deficit conditions (normal, wet or dry) of current-hydrological years, and (2) subdividing the water deficit conditions of the target year into 7 groups while keeping the non-target years with normal water condition (data inclusion criterion) (see Table S2 and Fig. S3 for more details).

For key step (1), we defined three classes of water deficit conditions: normal ($-\frac{1}{2}SD \leq D_{ya} \leq \frac{1}{2}SD$), wet ($D_{ya} > SD$), and dry ($D_{ya} < -SD$), in which SD was the standard deviation of annual water deficit anomalies (D_{ya}) with its corresponding tree-ring chronology. Under each of the three water deficit conditions of the current-hydrological years, we conducted key step (2). In order to study the legacy effect of a target year (the n^{th} ybc (with $n = 3, 2, 1$)), we controlled the water deficit condition of non-target years as normal through only including tree-ring specimens that met this criterion. To reveal the legacy effects of the n^{th} ybc (with $n = 3, 2, 1$), we subdivided tree ring specimens into

seven groups using water deficit of the n^{th} ybc (the cut off values were $D_{y,a} = -2SD, -SD, -1/2SD, 1/2SD, SD, 2SD$) (Figure S3a–3d). For each group, we calculated averages for RWIs and averages for $D_{y,a}$ of the n^{th} ybc. If the regression of mean RWIs of current-hydrological years over their corresponding mean water deficit of the n^{th} ybc were statistically significant (Figure S3b–3d), we would conclude that water deficit of the n^{th} ybc influenced current growth significantly. In this case, only normal water condition of the n^{th} ybc become the next inclusion criterion for tree-ring specimens when studying the legacy effect of its subsequent years. If the regression were not statistically significant (Figure S3a), then water deficit of the n^{th} ybc would be irrelevant for the subsequent selections of tree-ring specimens.

2.5.2. Calculation of water deficit legacy in tree-ring widths

Water deficit legacy (ΔRWI) was defined as a departure of the observed tree growth from expected growth (Anderegg et al., 2015). However, unlike the commonly used method which calculates “expected growth” based on the statistical relationship between growth or vegetation indices (e.g. RWI, NDVI) and climate variables (Anderegg et al., 2015; Jiang et al., 2019; Wu et al., 2017), we used control groups designated in the natural experiments to represent “expected growth” of trees (Eq. (5)).

$$\Delta RWI = RWI_O - RWI_C \quad (5)$$

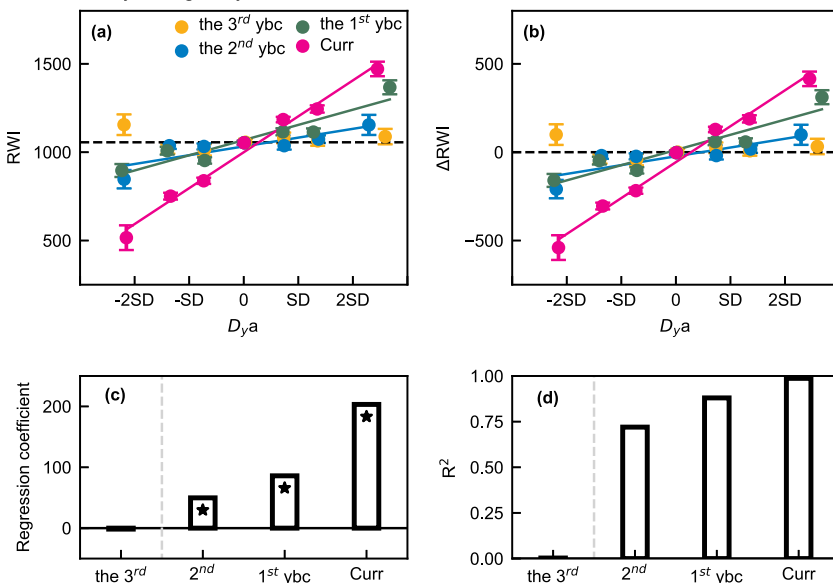
where RWI_O and RWI_C were the observed and expected regional mean forest growth, respectively.

Control groups (i.e. RWI_C), which represented the expected mean tree radial growth occurring in the absence of impacts from past water deficit, were critical for inferring legacy effects in this study. Under each water deficit condition of current-hydrological years, we selected tree-ring specimens formed under the normal condition of antecedent hydrological years (i.e. years in which regression relationships between water deficit and growth legacies were statistically significant) as the control group.

2.5.3. To investigate the impacts of inter-annual water deficit on forest coverage

We used FCC data to further study the impacts of inter-annual water deficit on forest coverage dynamics. We first set selection criteria (normal, wet or dry) to water deficit conditions of the current and its previous year, and then grouped FCC data according to those criteria so analysis could be conducted among those groups.

Current-hydrological years normal condition



2.6. Results validation

To validate our results, we used the bootstrap method to resample with replacement and established 1000 new databases, each of which also contained 29 969 RWI specimens. These new databases were used to repeat our analyses and these results are presented in Table S3.

3. Results

We built linear regressions of differing water deficit severity in different time periods against the current-hydrological years' RWI (Fig. 2a). By comparing with the control group of the current-hydrological years normal condition, we calculated averaged water deficit impacts on tree-rings for each level of water deficit in each hydrological year (Fig. 2b). The impact intensity of water deficit on tree radial growth changed across lag years. Additionally, in each lag year (i.e. the 3rd ybc, the 2nd ybc, the 1st ybc and current-hydrological years), the impact intensity increased as a function of the water deficit. The greatest regression coefficient of $RWI/\Delta RWI - D_{y,a}$ (i.e. the steepest slope of regression) occurred in current-hydrological years (magenta solid line in Figs. 2a, b), which suggested that water deficit conditions in current-hydrological years have the strongest impact on growth. As time recedes to prior years, the regression coefficients decreased from 203.3 to 86.0 and 49.8, respectively, which quantitatively described the decreasing water deficit legacies retained in tree-rings when going back to more remote past (Fig. 2c). Besides the direct impacts of current-hydrological years, legacy effects of 2 prior years were also significant ($p < 0.05$) when holding water deficit in current-hydrological years within normal range (Figs. 2c, d).

Since tree radial growth is most sensitive to water deficit in current-hydrological years, then the “superimposed effect”—i.e. the direct impact of water deficit on growth superimposed on water deficit legacy from antecedent years—cannot be neglected. Thus, we assigned RWI specimens formed under wet and dry conditions of current-hydrological years into different groups. Generally, tree radial growth benefited from the current wet conditions (RWI_C averaged 1282), and was constrained by current dry conditions (RWI_C averaged 705) (Fig. 3a,b and c). Water deficit legacies were stronger under the current dry conditions than that under the current wet conditions (Fig. 3d). Legacy effects of the 3rd ybc were tested significant when undergoing dry conditions in current-hydrological years, while under current-hydrological years wet conditions, only previous 1 year's legacy effects were tested significant, and

Fig. 2. Water deficit legacies of the 3rd (yellow), 2nd (blue) and 1st (green) years before current (magenta) years (ybc) under normal water condition of the current-hydrological years. Regressions of mean ring-width indices (RWIs) (a) or water deficit legacies (ΔRWI) (b) of current years over their corresponding mean water deficit of the n^{th} ybc. Regression coefficients (c) and determination coefficients (R^2) (d) of regressions in different time period. ΔRWI were calculated as the departure of averaged observed RWIs from the mean of control group ($RWI_C = 1056$); dashed black lines mark the mean of RWI_C ; error bars are means ± 1 SEM (standard errors of means). Regression coefficients with statistical significance ($p < 0.05$) were indicated with solid lines (a, b) and with asterisks (c). (For interpretation of the references to color in the text, the reader is referred to the web version of this article.)

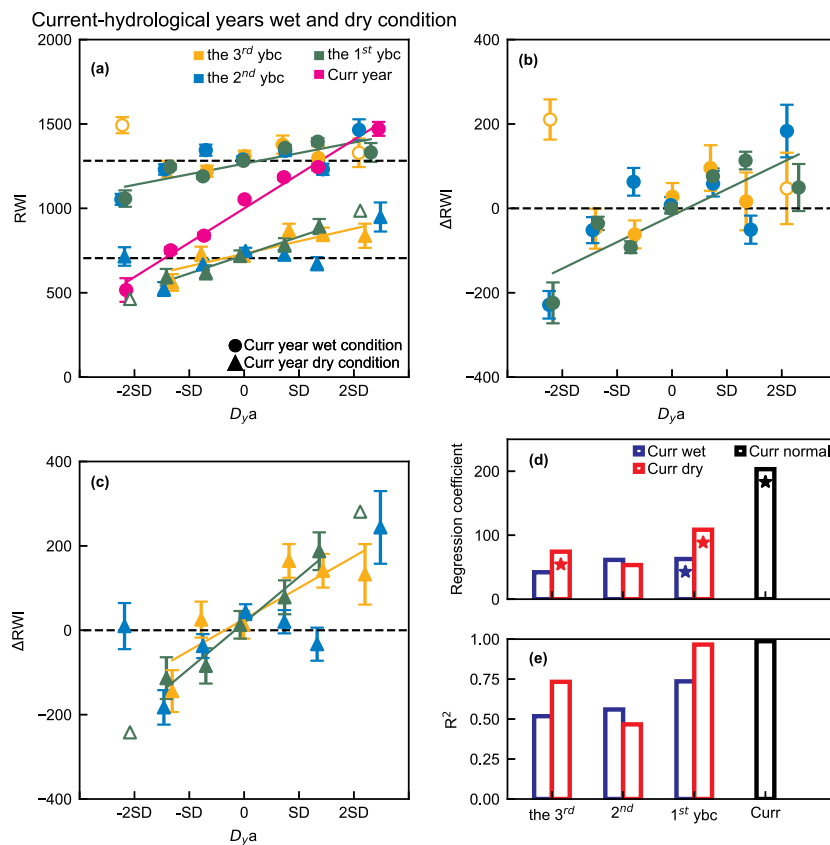


Fig. 3. Water deficit legacies of the 3rd (yellow), 2nd (blue) and 1st (green) years before current (magenta) years (ybc) under wet (circles in a, b) and dry (triangles in a, c) water conditions of the current-hydrological years. Regressions of mean ring-width indices (RWIs) (a) or water deficit legacies (ΔRWI) (b, c) of current years over their corresponding mean water deficit of the n^{th} ybc. Regression coefficients (d) and determination coefficients (R^2) (e) of regressions in different time period. ΔRWI were calculated as the departure of averaged observed RWIs from the mean of control group with current wet years (b, circles, $RWI_C = 1282$) or from the mean of control group with current dry years (c, triangles, $RWI_C = 705$), respectively; dashed black lines mark the mean of RWI_C ; error bars are means ± 1 SEM (standard errors of means). Regression coefficients with statistical significance ($p < 0.05$) were indicated with solid lines (a, b, c) and asterisks (d). (For interpretation of the references to color in the text, the reader is referred to the web version of this article.)

the intensity (indicated by regression coefficients) was only 57% of that under current-hydrological year dry conditions (Figs. 3d,e).

We further studied the impacts of inter-annual water deficit fluctuation on tree radial growth. As water condition of current-hydrological years improved, regardless of antecedent water conditions, the regional mean tree radial growth increased remarkably (Fig. 4a). In addition, tree radial growth further benefited from antecedent wetness but suffered negative impacts from antecedent dryness (Fig. 4a). Under each water deficit condition for the current-hydrological years, we conducted nonparametric tests (Mann-Whitney U test) between RWIs formed under the antecedent wet or dry conditions (blue or red dots in Fig. 4a) and RWIs formed under the antecedent normal conditions (black dots in Fig. 4a), which could be considered as treatment and control groups, respectively. All treatment groups were significantly different from their control groups ($p < 0.05$), except for the one in which trees experienced periods of consecutive dryness in both current and antecedent hydrological years (the bottom red dot in Fig. 4a). This suggested that consecutive years of dryness did not reduce the growth

of the surviving trees more than a single year of dryness in the study region.

By comparing with control groups, we calculated water deficit legacies. Antecedent wetness resulted in positive legacy effects yet antecedent dryness resulted in negative legacy effects (Fig. 4b); notably, the absolute values of positive legacy effects from antecedent wetness were generally larger than those of negative legacy effects from antecedent dryness, highlighting the extent of enhancement of antecedent wetness on individual tree growth. Positive legacy effects were most pronounced under the current-hydrological years' dry conditions, and least pronounced under the current-hydrological years' wet conditions; while negative legacy effects were most pronounced under the current-hydrological years' normal conditions, yet least pronounced under the current-hydrological years' dry condition.

The representativeness of tree radial growth to the changes of forest coverage is uncertain. To solve part of this uncertainty, we explored the impacts of inter-annual water deficit fluctuations on forest coverage. Under normal to wet conditions within 2-hydrological years, the

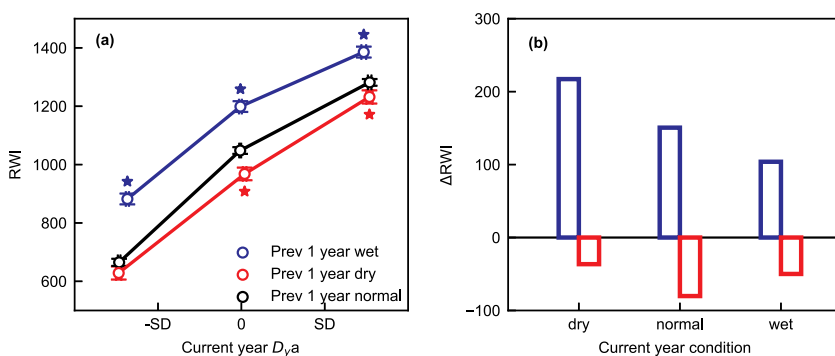


Fig. 4. Comparisons of water deficit legacies under different inter-annual water deficit conditions. (a) Averaged RWI under different inter-annual water deficit conditions. Tree-ring specimens formed under the wet or dry conditions in antecedent-hydrological years were selected as treatment groups (blue and red dots), and formed under normal conditions in antecedent-hydrological years were selected as control groups (black dots). Asterisks indicated treatment groups were significantly different from their control groups ($p < 0.05$). Sample size of each RWI group is given in Table S7. (b) Water deficit legacies (ΔRWI) under different water conditions of current-hydrological years. ΔRWI were calculated as the departure of the treatment groups (blue bars: wet in previous years; red bars: dry in previous years) from their control groups. (For interpretation of the references to color in the text, the reader is referred to the web version of this article.)

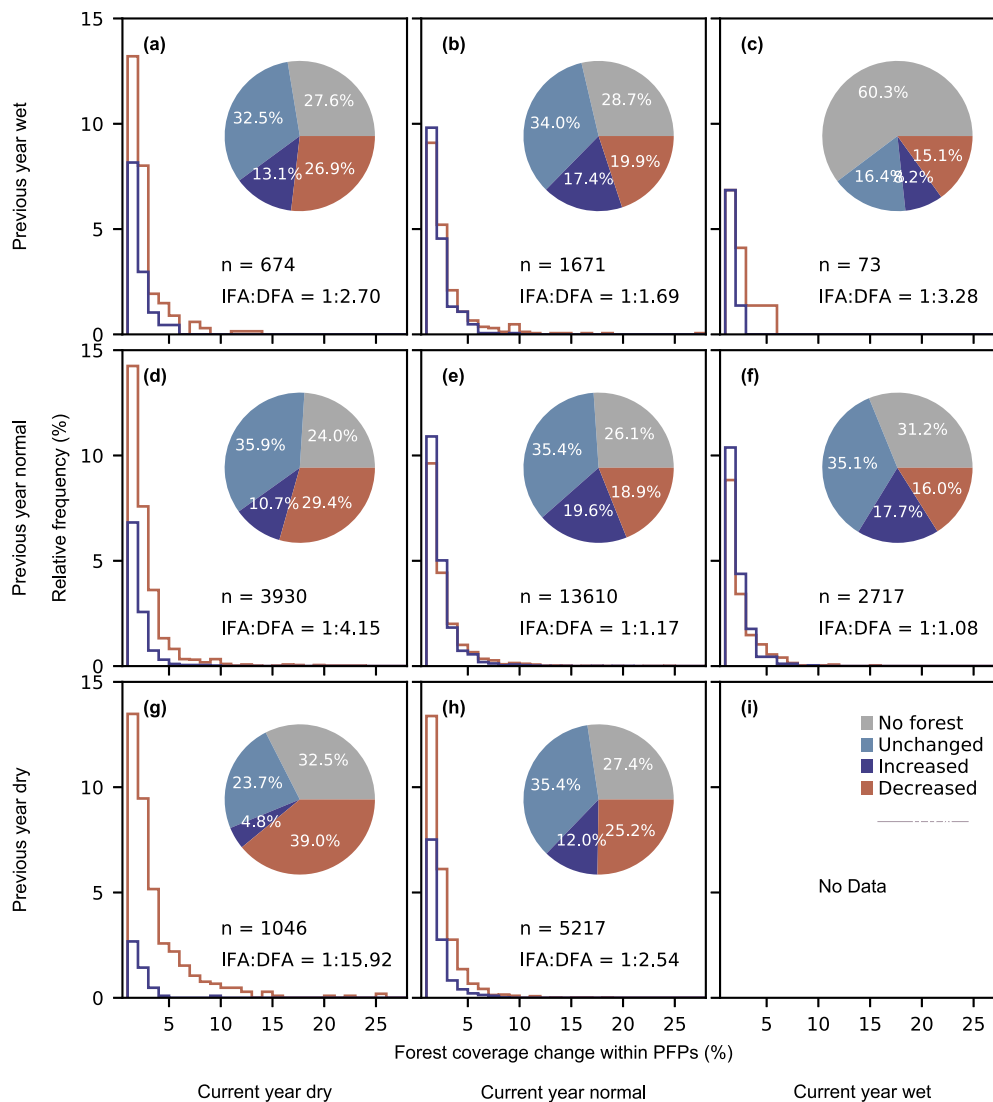


Fig. 5. The impact of inter-annual water condition on forest coverage change (FCC) within potential forest composited pixels (PFP) under wet-dry (a wet year followed by a current dry one, a), wet-normal (b), wet-wet (c), normal-dry (d), normal-normal (e), normal-wet (f), dry-dry (g), dry-normal (h), and dry-wet conditions (i). n is the number of pixels where inter-annual water deficit was consistent with the designed conditions. Pie plots present the percentages of pixels with no forest (gray), with forest coverage unchanged (turquoise), increased (blue) or decreased (red) forest coverage. “No forest” stand for the sub-pixel proportion of forest equal to zero in both current- and previous-hydrological years; “unchanged” stands for the sub-pixel proportion of forest larger than zero, yet FCC equal to zero; “increased” and “decreased” stands for positive and negative FCC, respectively. Increased forest area (IFA) and decreased forest area (DFA) are calculated as the accumulation of positive FCC and negative FCC, respectively. IFA: DFA represents the ratio of IFA to DFA. (For interpretation of the references to color in the text, the reader is referred to the web version of this article.)

proportion of pixels showing a decrease in forest coverage (i.e. negative FCC) was relatively small (pie plots in Figs. 5b,c,e,f), and the increased forest area (IFA) and decreased forest area (DFA) were comparable (histograms in Figs. 5b,e,f). This indicated that forest coverage remained relatively stable under normal to wet conditions. When experiencing dryness, the proportion of pixels corresponding to forest coverage decrease increased, whereas the proportion of pixels corresponding to forest coverage increase decreased (pie plots in Figs. 5a,d,g,h). Consequently, the ratio of IFA to DFA became smaller, especially under the consecutive dryness condition (histograms in Figs. 5a,d,g,h). This indicated that continuous dryness could lead to accelerated forest dieback.

4. Discussion

4.1. Temporal dynamics of water deficit legacy in tree-rings

In this study, we disentangled the impacts of water deficit on tree radial growth over a course of several years. Firstly, the impact of antecedent water deficit on radial growth of trees changed dynamically over time. The detectable impacts lasted, on average, for 1 to 3 hydrological years (close to 4 calendar years), and their duration strongly depended on water deficit conditions of current-hydrological years (Figs. 2c,3d). Secondly, the impact intensity of antecedent water

condition was affected not only by the amount of water deficit, but also by the elapsed time of water deficit and water deficit conditions of current-hydrological years (Figs. 2b,3b,3c). As shown in the results, $\Delta RWI-D_{y,a}$ regressions were tested significant in different time periods, but the intensity of legacy effects changed remarkably over those time periods (Figs. 2c,d, 3d,e). The results suggested that if we considered legacy effects to have constant intensity over a fixed timescale, uncertainties and bias could still arise when applying those statistical models to make forecasts.

The dynamic changes of water deficit legacy draw our attention to superimposed effects caused by current water deficit conditions. Under the dry conditions of current-hydrological years, tree radial growth was more easily affected by antecedent water deficit (Fig. 3c), and the detectable water deficit legacies lasted the longest (Fig. 3d). These results together with previous studies which found that drought legacies are most pronounced in arid ecosystems (Anderegg et al., 2015; D'Orangeville et al., 2018) indicate the importance of antecedent water conditions increased as vegetation faces more severe water shortage. In contrast, current wetness greatly benefits tree radial growth (Jiang et al., 2019; Peltier et al., 2016; Yi et al., 2018), and it diminishes the difference of legacy effects affected by antecedent water conditions. Moreover, the positive legacy effect via antecedent wetness was generally larger than the negative legacy effect from antecedent dryness (Fig. 4). This result demonstrates strong enhancement of wetness on

individual trees: antecedent wetness significantly enhanced resistance of individual trees to drought while wetness after drought accelerated their growth recovery.

For studying the temporal dynamics (i.e. the length, temporal patterns and strength) of legacy effects, we employed the natural experiment approach. A more frequently used analytic approach is the stochastic antecedent modeling (SAM) framework (Ogle et al., 2015). The SAM framework is mainly used to study the legacy effects after past extremes or disturbances, therefore, to identify those past events is the first step in the analyses. In this study, although we also studied the temporal dynamics of legacy effects, we emphasized the importance of current climate conditions, and our first step to conduct analyses is to differentiate the water deficit conditions (normal, wet or dry) of current-hydrological years, thus the SAM framework is less suitable. With the natural experiment designs, we compared legacy effects under different water deficit conditions of current years and observed the temporal dynamics of growth legacy. Natural experiment is a design-based approach, the statistical analyses of which are straightforward and transparent. Nevertheless, the representativeness of its results can be affected by the quantity and distribution of tree-ring sampling sites. Therefore, improving the representativity of the ITRDB will greatly benefit regional- to global-scale studies with tree-rings in the future (Zhao et al., 2018).

4.2. Comparisons of the impacts of inter-annual water deficit on tree growth and forest coverage

At landscape level, forest coverage will easily submit to dryness, but the recovery of it could not happen in a short period, and mainly stable inter-annual water deficit conditions may favor the recovery process in the study region. Comparing the dynamic changes between forest coverage and tree growth to inter-annual water deficit fluctuations, we can see some synchronized responses. After a dry year, both tree growth and forest coverage declined (Figs. 4,5a,5d,5h). This result is in line with other studies that as tree growth declines, dieback severity and mortality rate may increase in a region (Huang et al., 2015; Williams et al., 2010a). In recent decades, hotter droughts as well as increasingly severe wildfires and insect pests have pushed trees to the edge of survival (Anderegg et al., 2015b; Williams et al., 2012). Many studies reported the extensive drought-related tree mortality in the southwest USA (Meddens et al., 2015; van Mantgem et al., 2009). Therefore, the rapid and intense response of forest coverage within just two years not just reflect partial dieback of individual trees, but also the mortality of some trees and stands.

We also observed response differences to inter-annual water deficit fluctuation between forest coverage and individual trees. Unlike the sensitive response of tree radial growth to wetness, forest coverage remained relatively stable but did not expand under normal to wet inter-annual water deficit conditions within two years. This suggests that tree growth is more sensitive to wetness than forest coverage. To our surprise, when undergoing consecutive dry years, the decrease of forest coverage accelerated, yet the decline of tree growth showed no significant difference from it undergoing a single dry year. The representativeness of tree-ring data in the ITRDB has been questioned: some studies pointed out that tree-ring data in the ITRDB significantly overestimate regional forest climate sensitivity due to the specific selection of sampling sites (Klesse et al., 2018). Moreover, evidences showed that old and big trees are more sensitive and vulnerable under drought stress in the study region (Stovall et al., 2019; Xu et al., 2018). However, these findings cannot explain the difference between the response of tree growth and that of forest coverage, which were measured at different levels and with different resolutions, to persistent drought. A possible explanation is that trees sampled from environmentally harsh elevational range boundaries though climate sensitive are not subjected to strong competitive constraints (Anderegg and HilleRisLambers, 2019), indicating that competition for soil water is a

potent driver of tree mortality under a condition of persistent water shortage. Another explanation is that this result is an outcome of the “survivor bias” since tree-rings were sampled from surviving individuals which could be more resilient to drought stress. Updating more metadata (e.g., diameter at breast height, microenvironment information) of sampled trees in the ITRDB can help to clarify these uncertainties.

The differential and asymmetric impacts of dryness and wetness on tree growth and forest coverage may provide insights into the directional changes of forest ecosystems. When experiencing environmental stress, forest could manage multiple adjustments to reinforce their resilience (Trumbore et al., 2015), including enhancing physiological defenses (Tomioolo et al., 2017), reducing individual growth rates (Cailleret et al., 2017; Camarero et al., 2015; Coulthard et al., 2017; Lloret et al., 2011; Spannl et al., 2016), increasing resource-use efficiency (Zhang et al., 2014), compensating mortality through demographic stabilizing processes (Lloret et al., 2012), and altering community structure and species composition by increasing mortality or shifting dominance of tree species (Dorman et al., 2015; Kuparinen et al., 2010; Larson et al., 2015; van Mantgem et al., 2009; Young et al., 2017). When drought stress is relieved, compensatory growth of individuals occurred first, while the recovery of forest coverage may take more years under the premise of stable climate conditions.

Cross-scale comparisons of drought responses contribute to generating new insights of dynamic transitions of a forest under water stress. For instance, drought legacy effects were detected in tree-ring increments but not in other canopy processes in a deciduous broadleaf forest in Midwestern US, indicating that post-drought canopy allocation could be an important mechanism that decouples tree-ring signal from ecosystem fluxes (Kannenberg et al., 2019). Another case in point is that the decoupling of growing season length from wood biomass in drought-prone environments could be explained by the decrease of xylem growth rate under dryer climate (Ren et al., 2019; Ziaco and Liang., 2018). Therefore, linking the physiological processes of individuals and the ecological processes of an ecosystem is essential for integrating existing theories and further developing new theories.

5. Conclusions

To conclude, our results presented the dynamic and asymmetric impacts of inter-annual water deficit on both tree radial growth and forest coverage in the southwest USA. With abundant tree-ring records, forest coverage data and ad hoc designed natural experiments, we were able to study the temporal dynamics of legacy effects on multiple events, which is different from previous studies focusing on legacy effects of a single extreme event. In addition, we revealed that growth dynamics of individual trees do not fully represent forest-cover dynamics in response to drought. Tree-ring data are now being widely used to study climate impacts on forests due to their temporal continuity, spatial availability and accuracy in measurement, yet linking the variability of tree stem growth with processes involved in forest dynamics still needs efforts. Combining the study of individual trees and forest structure would enhance our ability of predicting future forest dynamic transitions under a rapidly changing climate.

Data statement

All data used are publicly and freely available online, and sources are noted in the text. Processed tree-ring data and climate data is attached in the supplementary data (Appendix B).

Declaration of Competing Interest

The authors declare that they have no known competing financial

interests or personal relationships that could have appeared to influence the work reported in this paper.

Acknowledgments

We acknowledge all the contributors to the International Tree-Ring Databank for tree-ring data. We thank the two anonymous reviewers for their constructive comments and suggestions for improving this manuscript. This study was supported by the National Natural Science Foundation of China (grant numbers 41571185 and 41621061), the Strategic Priority Research Program of Chinese Academy of Sciences (XDA20050101), the Fundamental Research Funds for the Central University (grant number 2015KJJC33), with additional financial support from the China Scholarship Council.

Supplementary materials

Supplementary material associated with this article can be found, in the online version, at doi:[10.1016/j.agrformet.2020.107980](https://doi.org/10.1016/j.agrformet.2020.107980).

References

- Allen, C.D., Betancourt, J.L., Swetnam, T.W., 1998. Landscape changes in the Southwestern United States: techniques, long-term data sets, and trends. In: Sisk, T.D. (Ed.), *Perspectives on the land use history of north America: A context for understanding our changing environment*. Lafayette, LA, pp. 71–84.
- Allen, C.D., Breshears, D.D., McDowell, N.G., 2015. On underestimation of global vulnerability to tree mortality and forest die-off from hotter drought in the Anthropocene. *Ecosphere* 6, 129–155. <https://doi.org/10.1890/ES15-00203.1>.
- Allen, C.D., Macalady, A.K., Chenchouni, H., Bachelet, D., McDowell, N., et al., 2010. A global overview of drought and heat-induced tree mortality reveals emerging climate change risks for forests. *Forest Ecol. Manag.* 259, 660–684. <https://doi.org/10.1371/journal.pone.0050755>.
- Anderegg, W.R.L., Kane, J.M., Anderegg, L.D.L., 2012. Consequences of widespread tree mortality triggered by drought and temperature stress. *Nat. Clim. Change* 3, 30–36. <https://doi.org/10.1038/npcas.1107891109>.
- Anderegg, W.R.L., Schwalm, C., Biondi, F., Camarero, J.J., Koch, G., et al., 2015. Pervasive drought legacies in forest ecosystems and their implications for carbon cycle models. *Science* 349, 528–532. <https://doi.org/10.1126/science.aab4097>.
- Anderegg, W.R., Hicke, J.A., Fisher, R.A., Allen, C.D., Aukema, J., et al., 2015b. Tree mortality from drought, insects, and their interactions in a changing climate. *New Phytol.* 208, 674–683. <https://doi.org/10.1111/nph.13477>.
- Anderegg, L.D.L., Hillerislambers, J., 2019. Local range boundaries vs. large-scale trade-offs: climatic and competitive constraints on tree growth. *Ecol. Lett.* 22, 787–796. <https://doi.org/10.1111/ele.13236>.
- Babst, F., Bodesheim, P., Charney, N., Friend, A.D., Girardin, M.P., et al., 2018. When tree rings go global: challenges and opportunities for retro- and prospective insight. *Quat. Sci. Rev.* 197, 1–20. <https://doi.org/10.1016/j.quascirev.2018.07.009>.
- Biederman, J.A., Scott, R.L., Bell, T.W., Bowling, D.R., Dore, S., et al., 2017. CO₂ exchange and evapotranspiration across dryland ecosystems of southwestern North America. *Global Change Biol.* 23, 4204–4221. <https://doi.org/10.1111/gcb.13686>.
- Cailleret, M., Jansen, S., Robert, E.M.R., Desoto, L., Aakala, T., et al., 2017. A synthesis of radial growth patterns preceding tree mortality. *Global Change Biol.* 23, 1675–1690. <https://doi.org/10.1111/gcb.13535>.
- Camarero, J.J., Gazol, A., Sangüesa-Barreda, G., Oliva, J., Vicente-Serrano, S.M., 2015. To die or not to die: early warnings of tree dieback in response to a severe drought. *J. Ecol.* 103, 44–57. <https://doi.org/10.1111/1365-2745.12295>.
- Camarero, J.J., Gazol, A., Sangüesa-Barreda, G., Cantero, A., Sanchez-Salguero, R., et al., 2018. Forest growth responses to drought at short- and long-term scales in Spain: squeezing the stress memory from tree rings. *Front. Ecol. Evol.* 6, 9. <https://doi.org/10.3389/fevo.2018.00009>.
- Cook, B.I., Ault, T.R., Smerdon, J.E., 2015. Unprecedented 21st century drought risk in the American southwest and central plains. *Sci. Adv.* 1, e1400082. <https://doi.org/10.1126/sciadv.1400082>.
- Cook, E.R., Briffa, K.R., Meko, D.M., Graybill, D.A., Funkhouser, G., 1995. The segment length curse in long tree-ring chronology development for paleoclimatic studies. *The Holocene* 5, 229–237. <https://doi.org/10.1177/095968369500500211>.
- Cook, E.R., 1985. *A Time Series Analysis Approach to Tree Ring Standardization*. University of Arizona, Tucson.
- Coulthard, B.L., Touchan, R., Anchukaitis, K.J., Meko, D.M., Sivrikaya, F., 2017. Tree growth and vegetation activity at the ecosystem-scale in the eastern Mediterranean. *Environ. Res. Lett.* 12, 84008. <https://doi.org/10.1088/1748-9326/aa7b26>.
- D'Orangeville, L., Maxwell, J., Kneeshaw, D., Pederson, N., Duchesne, L., et al., 2018. Drought timing and local climate determine the sensitivity of eastern temperate forests to drought. *Global Change Biol.* 24, 2339–2351. <https://doi.org/10.1111/gcb.14096>.
- Dorman, M., Svoray, T., Perevolotsky, A., Moshe, Y., Sarris, D., 2015. What determines tree mortality in dry environments? A multi-perspective approach. *Ecol. Appl.* 25, 1054–1071. <https://doi.org/10.1890/14-0698.1>.
- Dunning, T., 2008. Improving causal inference—strengths and limitations of natural experiments. *Polit. Res. Q.* 61, 282–293. <https://doi.org/10.1177/1065912907306470>.
- Dunning, T., 2012. *Natural Experiments in the Social Science—A Design-Based Approach*. Cambridge University Press.
- Fang, K., Frank, D., Zhao, Y., Zhou, F., Seppa, H., 2015. Moisture stress of a hydrological year on tree growth in the Tibetan Plateau and surroundings. *Environ. Res. Lett.* 10, 034010. <https://doi.org/10.1088/1748-9326/10/3/034010>.
- [Data set] Friedl, M., Sulla-Menashe, D., 2015. MCD12C1 MODIS/Terra + Aqua land cover type yearly L3 global 0.05Deg CMG V006. NASA Eosdis land processes DAAC. Accessed 2019-12-11 from 10.5067/MODIS/MCD12C1.006.
- Gao, S., Liu, R., Zhou, T., Fang, W., Chuixiang, Y., et al., 2018. Dynamic responses of tree-ring growth to multiple dimensions of drought. *Global Change Biol.* 24, 5380–5390. <https://doi.org/10.1111/gcb.14367>.
- Gazol, A., Camarero, J.J., Anderegg, W.R.L., Vicente-Serrano, S.M., 2017. Impacts of droughts on the growth resilience of Northern Hemisphere forests. *Global Ecol. Biogeogr.* 26, 166–176. <https://doi.org/10.1111/gcb.12526>.
- Hartmann, H., Moura, C.F., Anderegg, W.R.L., Ruehr, N.K., Salmon, Y., et al., 2018. Research frontiers for improving our understanding of drought-induced tree and forest mortality. *New Phytol.* 218, 15–28. <https://doi.org/10.1111/nph.15048>.
- Huang, K., Yi, C., Wu, D., Zhou, T., Zhao, X., et al., 2015. Tipping point of a conifer forest ecosystem under severe drought. *Environ. Res. Lett.* 10, 024011. <https://doi.org/10.1088/1748-9326/10/2/024011>.
- Huang, M., Wang, X., Keenan, T.F., Piao, S., 2018. Drought timing influences the legacy of tree growth recovery. *Global Change Biol.* 24, 3546–3559. <https://doi.org/10.1111/gcb.14294>.
- Jiang, P., Liu, H., Piao, S., Ciais, P., Wu, X., et al., 2019. Enhanced growth after extreme wetness compensates for post-drought carbon loss in dry forests. *Nat. Commun.* 10. <https://doi.org/10.1038/s41467-018-08229-z>.
- Kannenberg, S.A., Novick, K.A., Alexander, M.R., Maxwell, J.T., Moore, D.J.P., et al., 2019. Linking drought legacy effects across scales: From leaves to tree rings to ecosystems. *Global Change Biol.* 25, 2978–2992. <https://doi.org/10.1111/gcb.14710>.
- Klesse, S., DeRose, R.J., Guiterman, C.H., Lynch, A.M., Connor, C.D.O., et al., 2018. Sampling bias overestimates climate change impacts on forest growth in the southwestern United States. *Nat. Commun.* 9, 5336. <https://doi.org/10.1038/s41467-018-07800-y>.
- Kuparinen, A., Savolainen, O., Schurr, F.M., 2010. Increased mortality can promote evolutionary adaptation of forest trees to climate change. *For. Ecol. Manage.* 259, 1003–1008. <https://doi.org/10.1016/j.foreco.2009.12.006>.
- Larson, A.J., Lutz, J.A., Donato, D.C., Freund, J.A., Swanson, M.E., et al., 2015. Spatial aspects of tree mortality strongly differ between young and old-growth forests. *Ecology* 96, 2855–2861. <https://doi.org/10.1890/15-0628.1>.
- Leavitt, S.W., Woodhouse, C.A., Castro, C.L., Wright, W.E., Meko, D.M., et al., 2011. The North American monsoon in the U.S. Southwest: potential for investigation with tree-ring carbon isotopes. *Quat. Int.* 235, 101–107. <https://doi.org/10.1016/j.quaint.2010.05.006>.
- Liang, E., Leuschner, C., Dulamsuren, C., Wagner, B., Hauck, M., 2016. Global warming-related tree growth decline and mortality on the north-eastern Tibetan plateau. *Clim. Change* 134, 163–176. <https://doi.org/10.1007/s10584-015-1531-y>.
- Liu, S., Li, X., Rossi, S., Wang, L., Li, W., et al., 2018. Differences in xylogenesis between dominant and suppressed trees. *Am. J. Bot.* 105, 950–956. <https://doi.org/10.1002/ajb2.1089>.
- Lloret, F., Escudero, A., Iriondo, J.M., Martínez-Vilalta, J., Valladares, F., 2012. Extreme climatic events and vegetation: the role of stabilizing processes. *Global Change Biol.* 18, 797–805. <https://doi.org/10.1111/j.1365-2486.2011.02624.x>.
- Lloret, F., Keeling, E.G., Sala, A., 2011. Components of tree resilience: effects of successive low-growth episodes in old ponderosa pine forests. *Oikos* 120, 1909–1920. <https://doi.org/10.1111/j.1600-0706.2011.19372.x>.
- Meddens, A.J., Hicke, J.A., Macalady, A.K., Buotte, P.C., Cowles, T.R., et al., 2015. Patterns and causes of observed pinon pine mortality in the southwestern United States. *New Phytol.* 206, 91–97. <https://doi.org/10.1111/nph.13193>.
- McDowell, N.G., Allen, C.D., 2015. Darcy's law predicts widespread forest mortality under climate warming. *Nat. Clim. Change* 5, 669–672. <https://doi.org/10.1038/nclimate2641>.
- Ogle, K., Barber, J.J., Barron-Gafford, G.A., Bentley, L.P., Young, J.M., et al., 2015. Quantifying ecological memory in plant and ecosystem processes. *Ecol. Lett.* 18, 221–235. <https://doi.org/10.1111/ele.12399>.
- Peltier, D.M.P., Fell, M., Ogle, K., 2016. Legacy effects of drought in the southwestern United States: a multi-species synthesis. *Ecol. Monogr.* 86, 312–326. <https://doi.org/10.1002/ecm.1219>.
- Peltier, D., Ogle, K., 2019. Legacies of La Niña: north American monsoon can rescue trees from winter drought. *Global Change Biol.* 25, 121–133. <https://doi.org/10.1111/gcb.14487>.
- Preisler, Y., Tatarinov, F., Grünzweig, J.M., Bert, D., Ogée, J., et al., 2019. Mortality versus survival in drought-affected Aleppo pine forest depends on the extent of rock cover and soil stoniness. *Funct. Ecol.* 33, 901–912. <https://doi.org/10.1111/1365-2435.13302>.
- Reichstein, M., Bahn, M., Ciais, P., Frank, D., Mahecha, M.D., et al., 2013. Climate extremes and the carbon cycle. *Nature* 500, 287–295. <https://doi.org/10.1038/nature12350>.
- Ren, P., Ziaco, E., Rossi, S., Biondi, F., Prislán, P., et al., 2019. Growth rate rather than growing season length determines wood biomass in dry environments. *Agric. For. Meteorol.* 271, 46–53. <https://doi.org/10.1016/j.agrformet.2019.02.031>.
- Ryo, M., Aguilar-Trigueros, C.A., Pinek, L., Muller, L.A.H., Rillig, M.C., 2019. Basic principles of temporal dynamics. *Trends Ecol. Evol.* 34, 723–733. <https://doi.org/10.1016/j.tree.2019.03.007>.
- Salzer, M.W., Kipfmüller, K.F., 2005. Reconstructed temperature and precipitation on a

- millennial timescale from tree-rings in the southern Colorado Plateau. U.S.A. Clim. Change. 70, 465–487. <https://doi.org/10.1007/s10584-005-5922-3>.
- Spannl, S., Volland, F., Pucha, D., Peters, T., Cueva, E., et al., 2016. Climate variability, tree increment patterns and ENSO-related carbon sequestration reduction of the tropical dry forest species *Loxopterygium huasango* of Southern Ecuador. *Trees* 30, 1245–1258. <https://doi.org/10.1007/s00468-016-1362-0>.
- Stovall, A.E.L., Shugart, H., Yang, X., 2019. Tree height explains mortality risk during an intense drought. *Nat. Commun.* 10, 4385. <https://doi.org/10.1038/s41467-019-12380-6>.
- Swetnam, T.W., Betancourt, J.L., 1998. Mesoscale disturbance and ecological response to decadal climatic variability in the American Southwest. *J. Clim.* 11, 3128–3147. [https://doi.org/10.1175/1520-0442\(1998\)011<3128:MDAERT>2.0.CO;2](https://doi.org/10.1175/1520-0442(1998)011<3128:MDAERT>2.0.CO;2).
- Tomio, S., Metz, J., Blackwood, C.B., Djendouci, K., Henneberg, L., et al., 2017. Short-term drought and long-term climate legacy affect production of chemical defenses among plant ecotypes. *Env. Exp. Bot.* 141, 124–131. <https://doi.org/10.1016/j.envexpbot.2017.07.009>.
- Trumbore, S., Brando, P., Hartmann, H., 2015. Forest health and global change. *Science* 349, 814–818. <https://doi.org/10.1126/science.aac6759>.
- van Mantgem, P.J., Stephenson, N.L., Byrne, J.C., Daniels, L.D., Franklin, J.F., et al., 2009. Widespread increase of tree mortality rates in the western United States. *Science* 323, 521–524. <https://doi.org/10.1126/science.1165000>.
- Williams, A.P., Allen, C.D., Millar, C.I., Swetnam, T.W., Michaelsen, J., et al., 2010a. Forest responses to increasing aridity and warmth in the southwestern United States. *Proc. Natl. Acad. Sci. U.S.A.* 107, 21289–21294. <https://doi.org/10.1073/pnas.0914211107>.
- Williams, A.P., Allen, C.D., Macalady, A.K., Griffin, D., Woodhouse, C.A., et al., 2012. Temperature as a potent driver of regional forest drought stress and tree mortality. *Nat. Clim. Change* 3, 292–297. <https://doi.org/10.1038/nclimate1693>.
- Williams, A.P., Michaelsen, J., Leavitt, S.W., Still, C.J., 2010b. Using tree rings to predict the response of tree growth to climate change in the continental United States during the twenty-first century. *Earth Interact.* 14, 1–20. <https://doi.org/10.1175/2010EI362.1>.
- Wu, X., Liu, H., Li, X., Ciais, P., Babst, F., et al., 2017. Differentiating drought legacy effects on vegetation growth over the temperate Northern Hemisphere. *Global Change Biol.* 24, 504–516. <https://doi.org/10.1093/nsr/nwy158>.
- Xu, P., Zhou, T., Yi, C., Fang, W., Hendrey, G., et al., 2018. Forest drought resistance distinguished by canopy height. *Env. Res. Lett.* 13, 75003. <https://doi.org/10.1088/1748-9326/aacadd>.
- Yi, C., Mu, G., Hendrey, G., Vicente-Serrano, S.M., Fang, W., et al., 2018. Bifurcated response of a regional forest to drought. *Expert Opin. Environ. Biol.* 7, 1000153. <https://doi.org/10.4172/2325-9655.1000153>.
- Young, D.J.N., Stevens, J.T., Earles, J.M., Moore, J., Ellis, A., et al., 2017. Long-term climate and competition explain forest mortality patterns under extreme drought. *Ecol. Lett.* 20, 78–86. <https://doi.org/10.1111/ele.12711>.
- Ziaco, E., Liang, E., 2018. New perspectives on sub-seasonal xylem anatomical responses to climatic variability. *Trees* 33, 973–975. <https://doi.org/10.1007/s00468-018-1786-9>.
- Zhao, S., Pederson, N., D'Orangeville, L., Hillerislambers, J., Boose, E., et al., 2018. The international tree-ring data bank (ITRDB) revisited: data availability and global ecological representativity. *J. Biogeogr.* 46, 355–368. <https://doi.org/10.1111/jbi.13488>.
- Zhang, X., Susan Moran, M., Zhao, X., Liu, S., Zhou, T., et al., 2014. Impact of prolonged drought on rainfall use efficiency using Modis data across China in the early 21st century. *Remote Sens. Environ.* 150, 188–197. <https://doi.org/10.1016/j.rse.2014.05.003>.
- Zweifel, R., Eugster, W., Etzold, S., Dobbertin, M., Buchmann, N., et al., 2010. Link between continuous stem radius changes and net ecosystem productivity of a sub-alpine Norway spruce forest in the Swiss Alps. *New Phytol.* 187, 819–830. <https://doi.org/10.1111/j.1469-8137.2010.03301.x>.